CrossMark

The thermal decomposition of silver dinitramide $AgN(NO_2)_2$

Baili Chen[1] · Bo Jin[1] · Rufang Peng[1] · Fengqi Zhao[2] · Jianhua Yi[2] ·
Huijuan Guan[1] · Xingbing Bu[1] · Jun Zhao[1] · Shijin Chu[1]

Abstract Silver dinitramide $AgN(NO_2)_2$ was prepared, and its structure was characterized by UV–Visible absorption spectra, Fourier transform infrared (FT-IR) spectra and Fourier transform Raman spectra. Its thermal decomposition process was investigated by differential scanning calorimetry and thermogravimetric analysis coupled with the gas analysis by FT-IR (EGA-FT-IR). The intermediate and final products of thermal decomposition were analyzed by FT-IR, Raman spectra and X-ray diffraction. Kissinger method and Ozawa methods were used to calculate apparent activation energy E_a, the pre-exponential constant $\lg A$ and linear correlation coefficient r. The results showed that the degradation process of $AgN(NO_2)_2$ could be divided into two stages. The first one with a mass loss of 21.86 % took place in 408–483 K, in which N_2O was released and the intermediate product of thermal decomposition was $AgNO_3$. The second stage with a mass loss of 28.24 % occurred in 483–800 K. In this process, gases NO_2 and O_2 were evolved and Ag was the final product of thermal decomposition. Kissinger method results: $E_a = 66.59$ kJ mol^{-1}, $\lg A = 7.21$ min^{-1} and $r = 0.9913$. Ozawa method results: $E_a = 70.53$ kJ mol^{-1}, $r = 0.9987$.

✉ Bo Jin
jinbo0428@163.com

Baili Chen
chenbl@mail.ustc.edu.cn

Rufang Peng
rfpeng2006@163.com

1 State Key Laboratory Cultivation Base for Nonmetal Composites and Functional Materials, Southwest University of Science and Technology, Mianyang 621010, China

2 Xi'an Modern Chemistry Research Institute, Xi'an 710065, China

Introduction

Dinitramide salts were first discovered by American researchers in 1988 [1]. Since their initial report of the synthesis of dinitramide acid and dinitramide salts, the dinitramide salts have attracted intense attention [2–10]. A potential use of dinitramide salts is as an environment-friendly replacement for ammonium perchlorate. The application of dinitramide salts in composite solid propellants eliminates the emission of chlorinated exhaust products from rocket [5]. These salts have high oxygen density, high heat of formation and high densities [11]. They are promising candidates for highly energetic materials with potential industrial or military application. The main advantages of such salts are the high specific impulse, the high burning rates, less production of smoke and a cheaper price [12, 13]. Ammonium dinitramide (ADN) is the most well-known salts of dinitramide [11, 14] because of its superior performance in composite solid propellants. However, the application of ADN is restricted by a big problem of high moisture [15]. And many other metal ion salts, such as K^+, $Cu(NH_3)_4^+$ and $Pd(NH_3)^+$ as the cations, also have the same problem [16]. Numerous studies have exploited some organic ion salts of dinitramide to solve the problem [11, 14, 17]. The preparation of many new organic energetic salts of dinitramide needs appropriate dinitramide transfer reagents [18]. Free dinitramine $(HN(NO_2)_2)$ is one of dinitramide transfer reagents. $HN(NO_2)_2$ did not appear to be promising because of its instability, decomposing at 273.15 K [19]. Generally, silver dinitramide $(AgN(NO_2)_2)$ was used as the dinitramide transfer reagents [2, 16, 20, 21].

$AgN(NO_2)_2$ was first prepared through the metathesis reaction of potassium dinitramide (KDN) and silver nitrate in 1994 [19]. However, this compound was just characterized by melting point, elemental analysis [19], IR, Raman, ^{109}Ag and ^{14}N NMR [18]. The crystal structure of $AgN(NO_2)_2$ was reported in 2008 by Klapötke [22]. It is well known that $AgN(NO_2)_2$ is an energetic compound and an excellent dinitramide transfer reagent [23]. It is essential to have as much information as possible about the mechanism of the thermal decomposition, especially the products and energetics of each decomposition step. There are few reports about the thermal decomposition of $AgN(NO_2)_2$ up to date.

The main purpose of this work is to investigate the mechanism of the thermal decomposition of $AgN(NO_2)_2$ comprehensively. The thermal decomposition of $AgN(NO_2)_2$ was monitored by coupled DSC and TG/EGA-FTIR techniques under nitrogen atmosphere. The decomposition products were analyzed by UV–Vis, FT-IR, Raman and XRD techniques, and the thermodynamics analysis of its degradation was analyzed using Kissinger method and Ozawa method.

Experimental

Materials and instruments

Materials

Potassium hydroxide (AR), acetone (AR), amino acid (AR), isopropanol (AR), sulfuric acid (AR), silver nitrate (AR), ethanol (AR) and 95 % fuming nitric acid (industrial grade) were purchased from Cheng Du Kelong Chemical Co., Ltd. (China). Liquid nitrogen (99.99 %) was purchased from Mianyang Chang Jun Gas Co., Ltd. (China). All solvents were used without further purification.
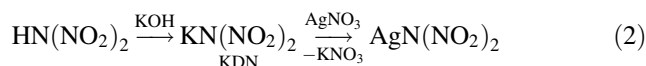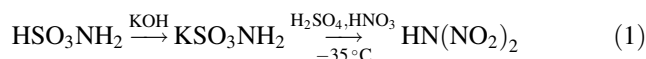
Instruments

UV–Vis spectra were measured with a UV-2102 PCS spectrometer using demonized water as solvent. IR spectra were recorded with a Nicolet 5700 spectrometer ($4000–400 \text{ cm}^{-1}$ with accuracy of recording 1 cm^{-1}) using KBr pellets. Raman spectra were recorded with an InVia spectrometer. TG measurements, coupled with the evolved gas analysis by FTIR (EGA-FTIR), were carried out with a TG209F1 instrument connected to a Nicolet 5700 FTIR spectrometer. $AgN(NO_2)_2$ sample (11.32 mg) was placed in a platinum crucible in the microbalance and was heated from room temperature to 1200 K. The analysis was performed under 90 mL min^{-1} supplied nitrogen flow and at a heating rate of 10 K min^{-1}. The gases released were introduced through a heated tube into a FTIR cell. The absorption

spectra were recorded in the region 4000–400 cm^{-1} with a resolution of 1 cm^{-1} by a Nicolet 5700 spectrometer to follow the progress of decomposition. Differential scanning calorimetric (DSC) curves of sample were recorded on a TA Q200 differential scanning calorimeter at heating of 5, 10, 15 and 20 K min^{-1} under nitrogen atmosphere. In the DSC, about 1.5 mg of sample was placed in an aluminum sample pan. The solid products of the thermal decomposition of $AgN(NO_2)_2$ were analyzed by XRD, Raman and FTIR techniques. The pure $AgNO_3$ (purchased from Cheng Du Kelong Chemical Co., Ltd. China) was analyzed by Powder X-ray diffraction (XRD) as reference. XRD patterns were recorded on an X'PERT PRO diffractometer, using Cu-K$_\alpha$-radiation. Room temperature diffract grams were recorded at scanning from 30° to 140°.

Synthesis

The synthesis route of $AgN(NO_2)_2$ is shown in Eqs. 1 and 2. Potassium dinitramide [$KN(NO_2)_2$, KDN] synthesis was carried out according to the literature [6] as the following procedure (reactions 1 and 2). $AgN(NO_2)_2$ was prepared by a modified procedure (reactions 1 and 2) according to the literature [18].

$$HSO_3NH_2 \xrightarrow{KOH} KSO_3NH_2 \xrightarrow[-35\,°C]{H_2SO_4, HNO_3} HN(NO_2)_2 \qquad (1)$$

$$HN(NO_2)_2 \xrightarrow[KDN]{KOH} KN(NO_2)_2 \xrightarrow[-KNO_3]{AgNO_3} AgN(NO_2)_2 \qquad (2)$$

The preparation of potassium sulfamate

Sulfamic acid (71.00 g) was suspended in 50.0 mL deionized water, and 50.0 mL 15.4 mol L^{-1} potassium hydroxide solution was added into the suspended sulfamic acid under stirring at room temperature. After adding potassium hydroxide solution, the mixture was kept stirring for 25 min until it became clear. Then the neutral solution was poured into 200.0 mL ethanol, and white solid precipitated. The precipitate was filtered on a filter paper and was washed three times with ethanol. Then solid product was dried in vacuum drying oven at 343 K, to obtain 83.50 g potassium sulfamate.

Under vigorous stirring, 17.00 g potassium sulfamate was gradually added into a 60 mL mixed acid system sulfuric acid–nitric acid (3:1, vol/vol). The nitric–sulfuric acid was kept cool from 238.15 to 228.15 K, with a mixture of liquid nitrogen and ethanol. The viscosity increased significantly as the reaction proceeded, and KHSO$_4$ precipitated. After reacting 25 min, the reaction mixture was poured into a bath including 300.0 g mixture of crushed ice and deionized water, and the cooled mixture was neutralized immediately with 200 mL 5.0 mol L^{-1} cold potassium hydroxide solution; during this process, the temperature of system must be

kept below 273 K. The solution became green-yellow when the neutralization approached its terminal point. The potassium hydroxide solution was kept adding into reaction mixture until the pH of solution equaled 8.

The reaction mixture was concentrated by a rotary evaporator until the mixture became dry powder. And the latter was extracted with 150 mL acetone, and the unsolvable solid was filtered. The acetone solution was concentrated with an evaporator to about one-tenth of volume and was poured into 120 mL 2-propanol. The precipitated salt was filtered and dried in vacuum oven at 343 K to obtain 9.3 g KDN, with a yield rate of 53 %.

The preparation of AgN(NO₂)₂

KDN (1.45 g) was dissolved in 100 mL of boiling ethanol, and 1.70 g AgNO₃ was dissolved in 100 mL of boiling ethanol. The above two boiling solutions were mixed, and KNO₃ was precipitated. When the system was cooled to 293 K, KNO₃ was filtered from the solution. The filtrate was concentrated in a rotatory evaporator to about one-fifth of the initial volume, and some impurity precipitated. The impurity was filtrated while hot. The filtrate was evaporated to dryness to obtain yellow crystals 1.75 g AgN(NO₂)₂, with a yield of 82 %.

Results and discussion

Sample characterization

The UV–Vis spectra of AgN(NO₂)₂ in water are shown in Fig. 1. It was shown that the aqueous of AgN(NO₂)₂ exhibited intense bands at 212 and 284 nm and a band of low intensity (a shoulder) at 335 nm, which corresponded to the dinitramide anion [24].
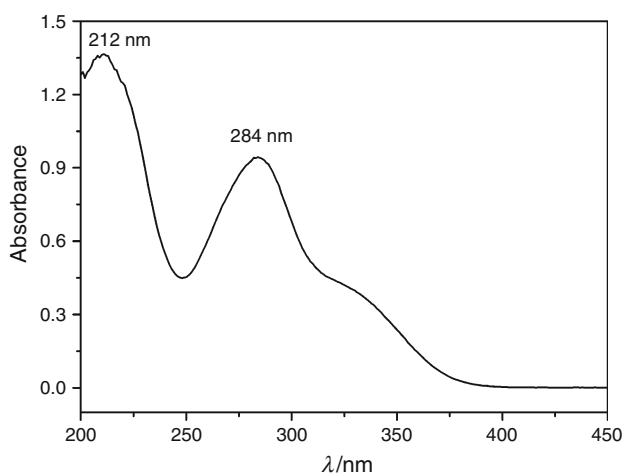
The Raman spectra of AgN(NO₂)₂ are shown in Fig. 2. Characteristic absorption peaks at 1506 and 1423 cm^{-1} in the Raman spectra were attributed to –NO₂ asymmetric stretching vibrations. The peaks at 1317, 1191, 1172 and 1121 cm^{-1} were ascribed to –NO₂ symmetric stretching vibrations. Bands at 1039 and 970 were related to group N₃ asymmetric and symmetric stretching vibrations, respectively. The peaks at 831, 754 and 493 were identified as –NO₂ flexural vibrations. The Raman spectra of AgN(NO₂)₂ were in accordance with the literature [25].

The IR spectra of AgN(NO₂)₂ are shown in Fig. 3. Characteristic absorption peaks at 1536 and 1431 cm^{-1} in the IR spectra were attributed to –NO₂ anti-symmetric stretching vibrations. The peaks at 1384, 1344, 1205 and 1178 cm^{-1} were ascribed to –NO₂ symmetric stretching vibrations. Bands at 1032 and 953 cm^{-1} were related to group N₃ anti-symmetric and symmetric stretching vibrations, respectively. The peaks at 827, 732, 762 and
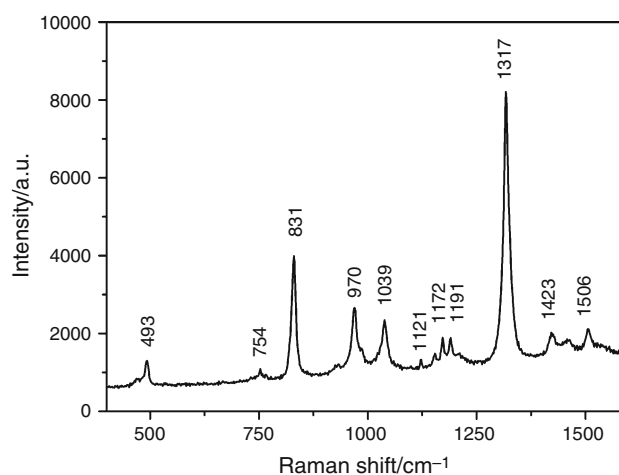

Fig. 2 Raman spectra of AgN(NO₂)₂

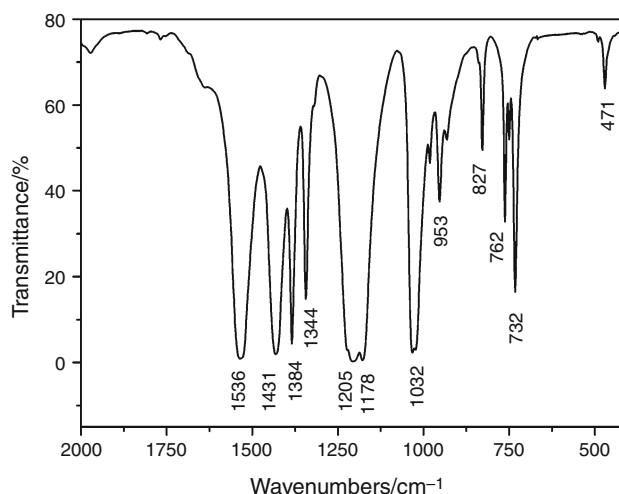**Fig. 1** UV–Vis spectra of silver dinitramide

Fig. 3 FT-IR spectra of AgN(NO₂)₂

Table 1 IR and Raman data of $AgN(NO_2)_2$

Approx. mode description	IR/cm^{-1}	Raman/cm^{-1}
v_{as} NO$_2$ in phase	1536	1506
v_s NO$_2$ in phase	1384	1317
	1344	
v_s N$_3$	953	970
δ_{sciss} NO$_2$ in phase	827	831
v_{as} NO$_2$ out of phase	1431	1423
v_s NO$_2$ out of phase	1205	1191
	1178	1172
		1121
v_{as} N$_3$	1032	1039
δ_{rock} NO$_2$ out of phase	732	754
δ_{wag} NO$_2$	471	493

Fig. 4 TG curves for $AgN(NO_2)_2$ at heating rate of 10 K min^{-1} under nitrogen

471 cm^{-1} were identified as –NO$_2$ flexural vibrations. Raman and IR data for $AgN(NO_2)_2$ assignment are presented in Table 1. The vibration data (Raman, IR) were in good agreement with the previously reported literature [6, 25]. Above discussions revealed that the sample contained $N(NO_2)_2^{-1}$. The melting point of $AgN(NO_2)_2$ was 405 K (Fig. 5), which was consistent with the Ref. [24]. Combining the analysis of FTIR, Raman with TG, the structure of $AgN(NO_2)_2$ can be confirmed.

Thermal decomposition of silver dinitramide

Thermal decomposition behavior is very important for energetic compounds. In order to get better understanding about thermal decomposition of $AgN(NO_2)_2$, TG and DSC methods were adopted to study the decomposition behaviors of $AgN(NO_2)_2$.

Figures 4 and 5 showed the TG and DSC curves for $AgN(NO_2)_2$ at a heating rate of 10 K min^{-1} in nitrogen atmosphere, respectively. As shown in Fig. 4, the decomposition process of $AgN(NO_2)_2$ could be divided to two stages. The first stage took place in 408–483 K with a mass loss of 21.86 %. It could be visualized in DSC curve (Fig. 5) that there was an endothermic peak at 405 K, which was attributed to the melt of $AgN(NO_2)_2$ [24]. It started to decompose at 407.5 K. A big exothermic peak at 437.7 K could be found, which indicated that a tremendous amount of heat was released quickly during the compound decomposing. The second stage with a mass loss of 28.24 % took place in 483–800 K. It started to lose mass at 523 K. It also could be observed in DSC curve that there was an endothermic peak appearing at about 625 K. It explained that some substance decomposed or sublimated, observing the mass losing from TG curve. A big endothermic peak appeared at 714 K, which may be
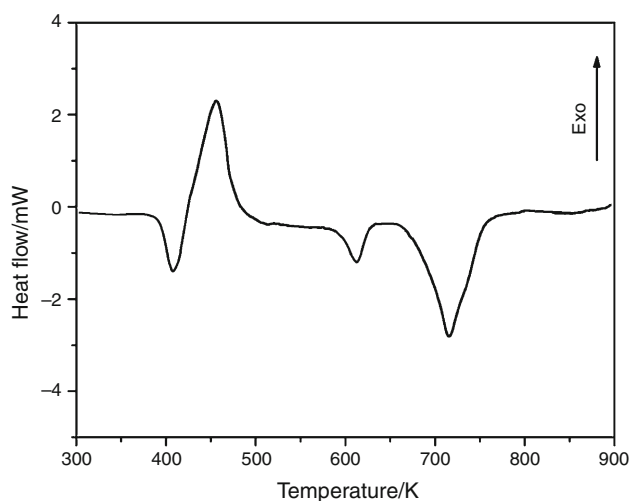
Fig. 5 DSC curve of $AgN(NO_2)_2$ at heating rate of 10 K min^{-1} under nitrogen

ascribed to the decomposition of silver nitrate according to the references [26, 27].

To investigate the proposed mechanism of decomposition of $AgN(NO_2)_2$, TG, EGA-IR, Raman and XRD technology were employed. The gases released from $AgN(NO_2)_2$ thermal decomposition were detected simultaneously by FT-IR spectroscopy (EGA-IR). The EGA-IR analysis results are shown in Fig. 6. It was observed that N$_2$O (1985 cm^{-1}) appeared in the first stage. The maximum evolution of N$_2$O (1985 cm^{-1}) was peaked at around 462 K. NO$_2$ (1380 cm^{-1}) forms in the second stage. The amount of released NO$_2$ reached the maximum at ∼760 K. These results manifested that NO$_2$ (1380 cm^{-1}) and N$_2$O were the main evolved gases.

In order to study the solid product of the $AgN(NO_2)_2$ decomposition, FT-IR, Raman and XRD techniques were used. The $AgN(NO_2)_2$ was heated up to 490 K and cooled

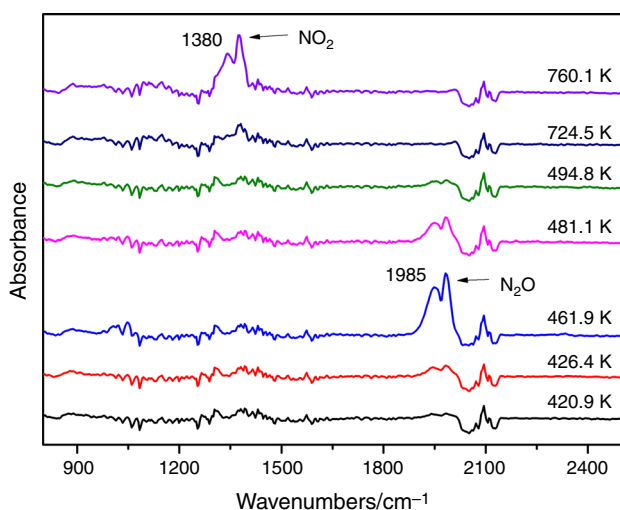**Fig. 6** IR spectra of gas products formed in the thermal decomposition of AgN(NO$_2$)$_2$

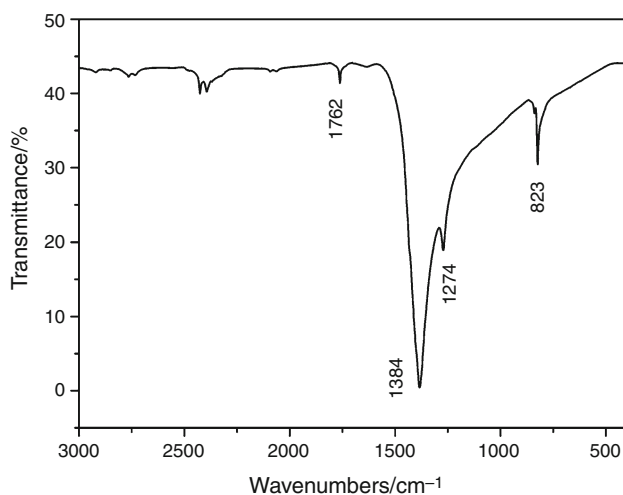**Fig. 7** FT-IR spectra of residues of AgN(NO$_2$)$_2$ after 490 K

Fig. 8 Raman spectra of residues of AgN(NO$_2$)$_2$ after 490 K (*a*) and pure AgNO$_3$ (*b*)
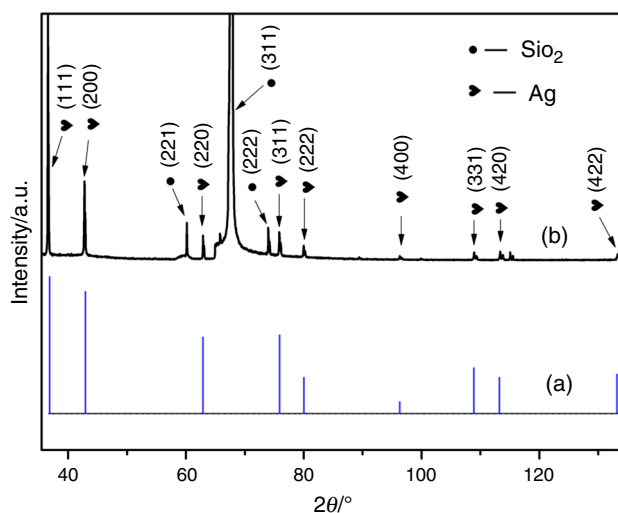
Fig. 9 The XRD diffraction patterns of Ag (*a*) and residues of AgN(NO$_2$)$_2$ after 873 K (*b*)

down to room temperature in nitrogen atmosphere, and the solid residue was analyzed with FT-IR and Raman detector. The FT-IR and Raman results are shown in Figs. 7 and 8a, respectively. In Fig. 7, characteristic bands of NO$_3^-$ were observed at 1762, 1384, 1274 and 823 cm^{-1}. The strong peaks at 1384 and 1274 cm^{-1} were related to asymmetric NO$_3^-$ stretching vibrations. The peak at 823 was ascribed to NO$_3^-$ symmetric bending vibrations. The peak observed at 1762 cm^{-1} was attributed to the combination bands (as a result of $v_1 + v_4$, the symmetric stretching and in-plane bending modes) of the nitrate ion [28]. It suggested that the solid residue was nitrate. However, the weak absorption peak at $\sim$2369 cm^{-1} was attributed to the symmetric stretching vibrations of CO$_2$, which was adsorbed by sample.

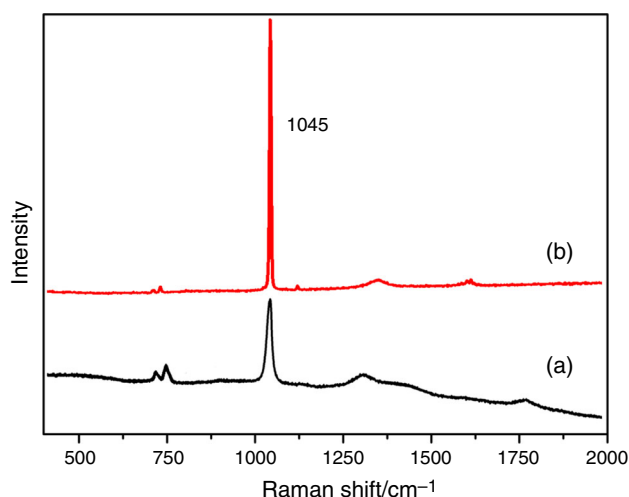The Raman spectra of pure AgNO$_3$ solid (purchased from Cheng Du Kelong Chemical Co., Ltd. China) are shown in Fig. 8b. The peaks at $\sim$1045, $\sim$1370 and $\sim$723 cm^{-1} could be observed in Fig. 8a, b. The NO$_3^-$ symmetric stretching band peak appeared at $\sim$1045 cm^{-1} and the asymmetric stretching appeared at $\sim$1370 cm^{-1} [29]. The above analysis indicated that AgNO$_3$ was the solid product of AgN(NO$_2$)$_2$ in first stage decomposition.

The AgN(NO$_2$)$_2$ was heated up to 873 K and cooled down to room temperature in nitrogen atmosphere, and the solid residue was analyzed by XRD. The result is shown in Fig. 9b. As shown in Fig. 9b, all detectable peaks were indexed as the SiO$_2$ and Ag with structure comparable to the standard data PDF no. 80-2157 (SiO$_2$) and PDF no.

00-004-0783(Ag), respectively. Therefore, the above analysis indicated that the Ag was the solid products of decomposition in second stage.

Based on the above analysis of TG (Fig. 4) and DSC curves (Fig. 5), the mass loss 21.86 % of the first decomposition was close to the theoretical mass loss calculated for the decomposition $AgN(NO_2)_2$ to $AgNO_3$ and N_2O (20.56 %). The mass loss 28.24 % of the second
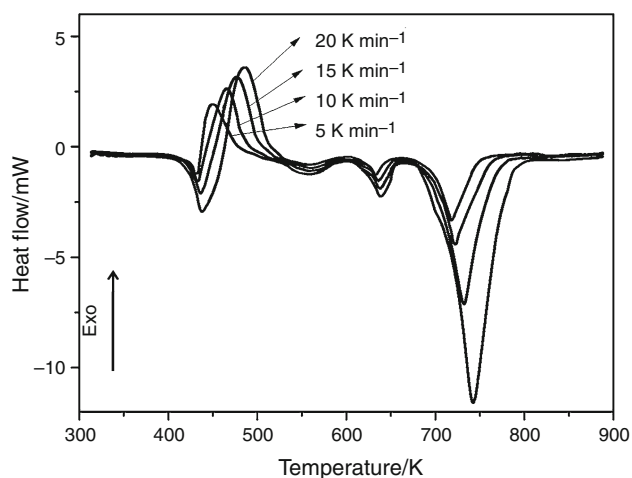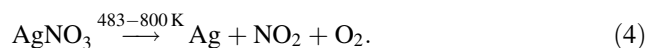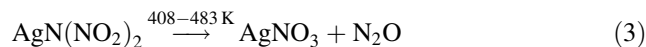

Fig. 10 DSC curves of $AgN(NO_2)_2$ at heating rates of 5, 10, 15 and 20 K min^{-1}

Table 2 Decomposition temperature T_p, $1/T_p$, ln (β/T_p^2) for thermal behavior of $AgN(NO_2)_2$ at different heating rates

Heating rate β/ K min^{-1}	The first peak of DSC curve T_p/K	$1/T_p$/K^{-1}	ln (β/T_p^2)
5	441.16	0.002267	−10.5694
10	455.36	0.002196	−9.9396
15	464.76	0.002151	−9.5750
20	473.97	0.002110	−9.3266

decomposition was close to the total mass loss expected for the conversion of $AgNO_3$ to NO_2, Ag and O_2 (29.91 %). The EGA-IR analysis (Fig. 6), IR (Fig. 7) and Raman (Fig. 8) analysis revealed that the main products of $AgN(NO_2)_2$ decomposition were $AgNO_3$ and N_2O in first stage (408–483 K). The thermal decomposition of $AgN(NO_2)_2$ in the first decomposition could be described by reaction 3. The EGA-IR analysis (Fig. 6) and XRD analysis proved that Ag and NO_2 were the main products in the second decomposition stage. Taking the EGA, XRD analysis and thermal analysis into account, the intermediate decomposition product $AgNO_3$ decomposed into Ag, O_2 and NO_2 in 483–800 K in nitrogen atmosphere. In the literature, the decomposition of $AgNO_3$ was studied in argon and artificial atmosphere. It was proved that Ag, O_2 and NO_2 were the decomposition product of $AgNO_3$ [28]. Therefore, the degradation of intermediate decomposition product $AgNO_3$ could be described by reaction 4. Therefore, the mechanism of decomposition of $AgN(NO_2)_2$ could be proposed (Eqs. 3 and 4):

$$AgN(NO_2)_2 \xrightarrow{408-483\,K} AgNO_3 + N_2O \qquad (3)$$

$$AgNO_3 \xrightarrow{483-800\,K} Ag + NO_2 + O_2. \qquad (4)$$

Thermal decomposition kinetics of silver dinitramide

To further understand the thermal decomposition behavior of silver dinitramide, Kissinger [30, 31] method and Ozawa method [32, 33] were employed to calculate the exothermal decomposition reaction kinetic parameters [apparent activation energy E_a (kJ mol^{-1}) and the pre-exponential constant A (min^{-1})] of $AgN(NO_2)_2$. In the temperature range 298–873 K, the DSC curves of silver dinitramide at heating rates of 5, 10, 15 and 20 K min^{-1} are shown in Fig. 10. In
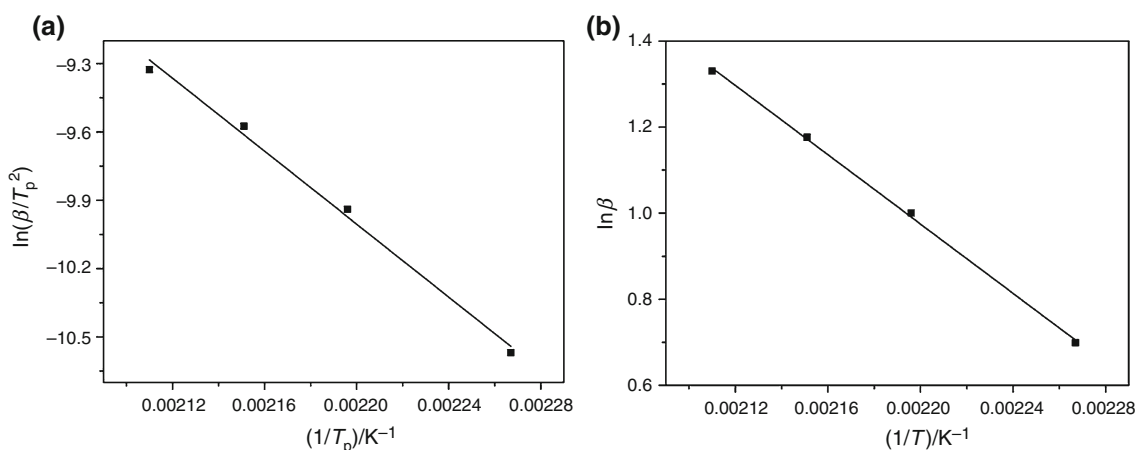

Fig. 11 Linear relationships of ln (β/T_p^2) and $1/T_p$ (**a**) and linear relationships of lg β and $1/T$ (**b**)

Table 3 Kinetics parameters of thermal decomposition of AgN(NO₂)₂ calculated by Kissinger and Ozawa method

Methods	Activation energy, E_a/kJ mol^{-1}	Frequency factor, lg A/min^{-1}	Linear regression, r
Kissinger method	66.59	7.21	0.9913
Ozawa method	70.53		0.9987

Fig. 10, it could be easily observed that the decomposition temperature moved toward high temperature as the heating rate increased. The basic data for exothermic decomposition of AgN(NO₂)₂ are listed in Table 2.

Kissinger method was used to calculate activation energy:

$$\ln\left[\beta/T_p^2\right] = \ln[AR/E_a] - \left[E_a/(RT_p)\right]. \tag{5}$$

β is the heating rate (K min^{-1}), T_p is the decomposition temperature (K), E_a is the apparent activation energy (kJ mol^{-1}), A is the pre-exponential factors, and R is the ideal gas constant.

The relationships between $\ln[\beta/T_p^2]$ and $1/T_p$ were evaluated with linear regression analysis, which is shown in Fig. 11a. The activation energy was calculated from the relation between $\ln[\beta/T_p^2]$ and $1/T_p$, $E_a = 66.59$ kJ mol^{-1}, pre-exponential factors, $A = 16260816$, lg $A = 7.21$ min^{-1}, correlation coefficient, linear correlation coefficient, $r = 0.9913$.

Ozawa method was used to calculate activation energy:

$$\lg \beta = \lg[AE_a/RG(\alpha)] - 2.315 - 0.4567E/RT. \tag{6}$$

The relationships between lg β and $1/T$ were evaluated with linear regression analysis, which is shown in Fig. 11b. The activation energy was calculated from the relation between lg β and $1/T$, $E_a = 70.53$ kJ mol^{-1}, correlation coefficient, linear correlation coefficient, $r = 0.9987$.

The kinetics parameters of thermal decomposition of AgN(NO₂)₂ calculated by Kissinger and Ozawa methods are listed in Table 3. It could be easily concluded from Table 3 that values of E_a and lg$A$ calculated by Kissinger's method were in approximate agreement with the values calculated using Ozawa method. This meant that one could use either of Eqs. (4) and (5) to calculate the active energy of thermal decomposition.

Conclusions

The thermal decomposition behavior of AgN(NO₂)₂ was studied by DSC, TG, EGA, Raman, FT-IR and XRD. Its thermal decomposition could be divided into two stages:

the first stage (408–483 K) with a mass loss of 21.86 % and the second stage (483–800 K) with a mass loss of 28.24 %. The first stage gaseous decomposition product is N₂O, and solid decomposition product is AgNO₃. The second stage gaseous decomposition products are NO₂ and O₂, and solid decomposition product is Ag. The mechanism of decomposition of AgN(NO₂)₂ was proposed.

Apparent activation energy $E_a = 66.59$ kJ mol^{-1}, the pre-exponential constant lg $A = 7.21$ min^{-1} and linear correlation coefficient, $r = 0.9913$, were calculated by Kissinger method. $E_a = 70.53$ kJ mol^{-1} and $r = 0.9987$ were calculated by Ozawa method.

References

1. Venkatachalam S, Santhosh G, Ninan KN. An overview on the synthetic routes and properties of ammonium dinitramide (ADN) and other dinitramide salts. Propellants Explos Pyrotech. 2004; 3(29):178–87.
2. Klapötke TM, Mayer P, Schulz A, Weigand JJ. 1,5-Diamino-4-methyltetrazolium dinitramide. J Am Chem Soc. 2005; 127(7):2032–3.
3. Galvez-Ruiz JC, Holl G, Karaghiosoff K, Klapötke TM, Löhnwitz K, Mayer P, Nöth H, Polborn K, Rohbogner CJ, Suter M, Weigand JJ. Derivatives of 1,5-diamino-1H-tetrazole: a new family of energetic heterocyclic-based salts. Inorg Chem. 2005;44(12):4237–53.
4. Gilardi R, Flippenanderson J, George AC, Butcher RJ. A new class of flexible energetic salts: the crystal structures of the ammonium, lithium, potassium, and cesium salts of dinitramide. J Am Chem Soc. 1997;119(40):9411–6.
5. Bottaro JC, Penwell PE, Schmitt RJ. 1,1,3,3-Tetraoxo-1,2,3-triazapropene anion, a new oxy anion of nitrogen: the dinitramide anion and its salts. J Am Chem Soc. 1997;119:9405–10.
6. Chen BL, Jin B, Peng RF, Yi JH, Guan HJ, Bu XB, Chu SJ. Synthesis characterization and thermal decomposition of fullerene ethylenediamine dinitramide. Chin J Energy Mater. 2014;22: 467–72.
7. Fischer N, Joas M, Klapötke TM, Stierstorfer J. Transition metal complexes of 3-amino-1-nitroguanidine as laser ignitible primary explosives: structures and properties. Inorg Chem. 2013;52(23): 13791–802.
8. Xiao LB, Zhao FQ, Luo Y, Xing XL, Gao HX, Li N, Li X, Hu RZ. Dissolution properties of ammonium dinitramide in N-methyl pyrrolidone. J Therm Anal Calorim. 2014;117(1):517–21.
9. Zhang T, Li GX, Yu YS, Sun ZY, Wang M, Chen J. Numerical simulation of ammonium dinitramide (ADN)-based non-toxic aerospace propellant decomposition and combustion in a monopropellant thruster. Energy Convers Manag. 2014;87:965–74.
10. Klapötke TM, Schmid PC, Schnell S, Stierstorfer JJ. Thermal stabilization of energetic materials by the aromatic nitrogen-rich 4,4′,5,5′-tetraamino-3,3′-bi-1,2,4-triazolium cation 4,4′,5,5′-tetraamino-3,3′-bi-1,2,4-triazolium cation. J Mater Chem A. 2015; 3:2658–68.

11. Wingborg N, Latypov NV. Triaminoguanidine dinitramide, TAGDN: synthesis and characterization. Propellants Explos Pyrotech. 2003;28(6):314–8.

12. Singh RP, Verma RD, Meshri DT, Shreeve JM. Energetic nitrogen-rich salts and ionic liquids. Angew Chem Int Ed. 2006;45(22):3584–601.

13. Berger B, Bircher H, Studer M, Wälchli M. Alkali dinitramide salts. Part 1: synthesis and characterization. Propellants Explos Pyrotech. 2005;30(3):184–90.

14. Stmark H, Bemm U, Bergman H, Langlet A. N-guanylurea-dinitramide: a new energetic material with low sensitivity for propellants and explosives applications. Thermochim Acta. 2002;384(1):253–9.

15. Silva GD, Rufino SC, Iha K. Green propellants-oxidizers. J Aerosp Technol Manag. 2013;5(2):139–44.

16. Zeng Z, Wang R, Twamley B, Parrish DA, Shreeve JNM. Polyamino-substituted guanyl-triazole dinitramide salts with extensive hydrogen bonding: synthesis and properties as new energetic materials. Chem Mater. 2008;20(19):6176–82.

17. Fischer G, Holl G, Klapötke TM, Weigand JJ. A study on the thermal decomposition behavior of derivatives of 1,5-diamino-1H-tetrazole (DAT): a new family of energetic heterocyclic-based salts. Thermochim Acta. 2005;437(1–2):168–78.

18. Ang H, Fraenk W, Karaghiosoff K, Klap TM, Mayer P, Th HNO, Sprott J, Warchhold M. Synthesis, characterization, and crystal structures of Cu, Ag, and Pd dinitramide salts. Z Anorg Allg Chem. 2002;628(13):2894–900.

19. Luk'Yanov OA, Anikin OV, Gorlelik VP, Tartakovsky Tartakovsky VA. General and inorganic chemistry. Dinitramide and its salts. 3.8 metallic salts of dinitramide. Russ Chem Bull. 1994;43(9):1457–61.

20. Luk'Yanov OA, Jgevnin AR, Leichenko AA, Seregina NM, Tartakovsky VA. Organic chemistry dinitramide and its salts. 6.*dinitramide salts derived from ammonium bases. Russ Chem Bull. 1995;44(1):108–12.

21. Fischer N, Klapötke TM, Stierstorfer J. 1-Amino-3-nitroguani-dine (ANQ) in high-performance Ionic energetic materials. Z Naturforsch B: Chem Sci. 2012;67(6):573–88.

22. Klapötke TM, Krumm B, Scherr M. First structural characterization of solvate-free silver dinitramide, $Ag[N(NO_2)_2]$. Dalton Trans. 2008;43:5876–8.

23. Lei M, Liu ZR, Kong YH, Yin CM, Wang BZ, Wang Y. Zhang P. Thermochim Acta. 1999;335:113–20.

24. Shlyapochnikov EA, Cherskaya NO, Luk'Yanov OA, Gorelik EP, Tartakovsky ED. Dinitramide and its salts 4.* molecular structure of dinitramide. Russ Chem B. 1994;43(9):1522–5.

25. Christe KO, Wilson WW, Petrie MA, Michels HH, Bottaro JC, Gilardi R. The dinitramide anion, $N(NO_2)_2^-$. Inorg Chem. 1996;35(17):5068–71.

26. Lide DR. CRC handbook of chemistry and physics. 90th ed. Boca Raton: CRC Press; 2009 **(section 4 p:82)**.

27. Otto K, Acik IO, Krunks M, Tõnsuaadu K, Mere A. Thermal decomposition study of $HAuCl_4 \cdot 3H_2O$ and $AgNO_3$ as precursors for plasmonic metal nanoparticles. J Therm Anal Calorim. 2014;118(2):1065–72.

28. Dag Ö, Samarskaya O, Tura C, Günay A, Çelik Ö. Spectroscopic investigation of nitrate–metal and metal–surfactant interactions in the solid $AgNO_3/C_{12}EO_{10}$ and liquid-crystalline $[M(H_2O)_n](NO_3)_2/C_{12}EO_{10}$ systems. Langmuir. 2003;19(9):3671–6.

29. Balasubrahmanyam K, Janz GJ. Molten mixtures of $AgNO_3$ and $TlNO_3$: Raman spectra and structure. J Chem Phys. 1972;57:4089–91.

30. Kissinger HE. Reaction kinetics in differential thermal analysis. Anal Chem. 1957;29(11):1702–6.

31. Yang RT, Steinberg M. Differential thermal analysis and reaction kinetics for nth-order reaction. Anal Chem. 1977;49(7):998–1001.

32. Hu RZ, Shi QZ. Thermal analysis kinetics. Beijing: Science Press; 2001.

33. Yi JH, Zhao FQ, Xu SY, Zhang LY, Gao HX, Hu RZ. J Hazard Mater. 2009;165(1–3):853–9.